



Synthesis, Molecular Modeling of N-acyl Benzoazetinones and their Docking Simulation on Fungal Modeled Target

Inul Ansary, Arijit Das, Parth Sarthi Sen Gupta & Amal Kumar Bandyopadhyay

To cite this article: Inul Ansary, Arijit Das, Parth Sarthi Sen Gupta & Amal Kumar Bandyopadhyay (2017): Synthesis, Molecular Modeling of N-acyl Benzoazetinones and their Docking Simulation on Fungal Modeled Target, Synthetic Communications, DOI: [10.1080/00397911.2017.1328514](https://doi.org/10.1080/00397911.2017.1328514)

To link to this article: <http://dx.doi.org/10.1080/00397911.2017.1328514>



View supplementary material [↗](#)



Accepted author version posted online: 17 May 2017.



Submit your article to this journal [↗](#)



View related articles [↗](#)



View Crossmark data [↗](#)

Synthesis, Molecular Modeling of *N*-acyl Benzoazetinones and their Docking Simulation on Fungal Modeled Target

Inul Ansary¹, Arijit Das¹, Parth Sarthi Sen Gupta², Amal Kumar Bandyopadhyay²

¹Department of Chemistry, The University of Burdwan, Burdwan, W.B, India,

²Department of Biotechnology, The University of Burdwan, Burdwan, W.B, India

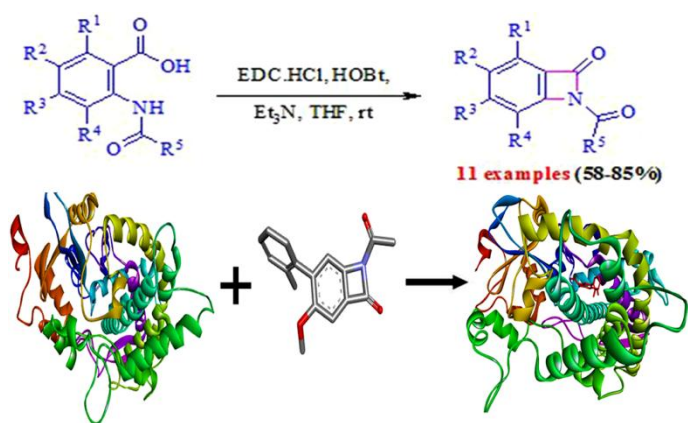
Corresponding to authors: Inul Ansary, Department of Chemistry, The University of Burdwan, Burdwan 713104, W.B, India; E-mail: iansary@chem.buruniv.ac.in; Amal Kumar Bandyopadhyay, Department of Biotechnology, The University of Burdwan, Burdwan 713104, W.B, India; E-mail: akbanerjee@biotech.buruniv.ac.in

Abstract

A series of stable *N*-acyl benzoazetinones have been synthesized in moderate to good yields (58-85%) from easily available substrates such as 2-(*N*-acyl) amino benzoic acids via intramolecular amidation under mild conditions. These geometry-optimized benzoazetinones were docked in the model target of P450, class CYP53A15, a benzoate 4-monooxygenase abundantly found in the genome of ascomycetes and basidiomycetes classes of pathogenic fungi. Low per residue RMSD of modeled structure of the enzyme indicated similar topology as template (4D6Z.pdb). Observed score judges site-specific docking, and the interaction of quantum mechanically optimized benzoazetinone derivatives with the target enzyme. These results suggest that **3i** is the best antifungal

agent. The specific hydrophobic substituent in the benzoazetinones contributed to the stability of ligand-target complex. Overall, the study provided insight into the specificity of the site-specific interactions, thereby, facilitating the possibility of development of broad-spectrum antifungal agents against opportunistic and infectious fungi.

GRAPHICAL ABSTRACT:



KEYWORDS: 2-(*N*-acyl) amino benzoic acids; EDC.HCl, HOBT; *N*-acyl benzoazetinones; molecular modeling; molecular docking

INTRODUCTION

Benzoazetinones is composed of β -lactam fused with a benzene ring. In recent years, β -lactam and its derivatives have been studied for their role in antibacterial activity^[1], synthesis of bioactive compounds^[2], enzymatic inhibitions,^[3] therapeutic applications,^[4, 5] and antifungal activities.^[6] Drug resistance^[7] led to the discovery of new drugs against invasive fungal infections^[8,9] caused by *Candida*,^[10] *Aspergillus*^[11] and *Colchilobus*,^[12] especially in immunocompromised patients.^[13] In this context, derivatives of amines, amides, and azoles were investigated for their antifungal activities against the target cytochrome-P450, CYP families.^[14] The latter are highly diverse in the genome of

fungi.^[15, 16] It is more so for the class CYP53A15 in the genome of pathogenic fungi and therefore, has been explored as a target for a wide variety of phenolic compounds.^[17] As a result, intensive investigations have been focused on β -lactam and its derivatives.^[18-20]

Several methods of synthesis of β -lactams have been reported in the recent past.^[21, 22] Since the synthesis of benzoazetines by photolysis^[23] and thermolysis^[24, 25] were reportedly unstable, either tertiary butyl^[26] or pivaloyl^[27, 28] was incorporated as an *N*-substituted group to improve its stability. However, the low yield of benzoazetines^[28, 29] and the presence of a by-product were also reported^[28]. Recently, Cioffi CL, et al. isolated stable benzoazetone as an intermediate starting from 2-(4-(2-(trifluoromethyl)phenyl)piperidine-1-carboxamido)benzoic acid during the synthesis of *N*-(2-(methylsulfonylcarbamoyl)phenyl)-4-(2-(trifluoromethyl)phenyl)piperidine-1-carboxamide.^[30]

Here, we report the synthesis of benzoazetines from easily available substrates 2-(*N*-acyl) amino benzoic acids via intramolecular amidation under mild conditions. Further, we carried out extensive investigations on optimization, three-dimensional structure, docking and site-specific interactions of these benzoazetines. The study also highlights the potentiality of CYP53A15 as a target for these compounds, thereby, allowing in gaining insight into the interactions at its active site. Since the crystal structure of CYP53A15 from *Cochliobolus lunatus* is unavailable, detailed homology modeling of CYP53A15 has also been worked out in the present study.

RESULTS AND DISCUSSION

Chemistry

The starting precursors, 2-(*N*-acyl)amino benzoic acids **2a-k**, were synthesized in 70-94% yields from the corresponding 2-amino benzoic acids **1a-j** by acylating with acyl chloride in the presence of Et₃N in THF at room temperature for 2 h (supporting information file).^[31]

We initiated our investigation with substrate **2a**, and the results are summarized in Table 1. When the substrate **2a** was subjected to react with 1.5 equiv of coupling reagent HATU (1-[Bis(dimethylamino)methylene]-1*H*-1,2,3-triazolo[4,5-*b*]pyridinium 3-oxide hexafluorophosphate) in the presence of 3.0 equiv of DIPEA (*N,N*-diisopropylethylamine) in DMF (*N,N*-dimethylformamide) at room temperature for 12 hours, only 15% yield of benzoazetinone **3a** was obtained (Table 1, entry 1)^[30]. To improve the yield of **3a**, the reaction was again carried out in the presence of Et₃N and pyridine, respectively. The former improved the yield compared with the latter (Table 1, entries 2 and 3). The yield of **3a** was further improved when the solvent DMF was substituted with THF (tetrahydrofuran) but not with DCM (dichloromethane) (Table 1, entries 4 and 5). Increase in HATU did not improve the yield of the product (Table 1, entry 6). Other coupling reagents such as DCC (dicyclohexylcarbodiimide), EDC.HCl (1-ethyl-3-(3-dimethylaminopropyl)carbodiimide hydrochloride), TBTU (2-(1*H*-benzotriazole-1-yl)-1,1,3,3-tetramethyluronium tetrafluoroborate) and HBTU (2-(1*H*-benzotriazol-1-yl)-1,1,3,3-tetramethyluronium hexafluorophosphate) were also tested, but the yield of **3a** was unsatisfactory (Table 1, entries 7-10). No product was obtained when

the coupling reagent PyBOP (benzotriazol-1-yloxy)tripyrrolidinophosphonium hexafluorophosphate) was used for an extended period of time (Table 1, entry 11). However, when the reaction was carried out with 1.5 equiv of DCC in the presence of 1.0 equiv of an additive HOBt (1-hydroxybenzotriazole) and 3.0 equiv of Et₃N in THF at room temperature for 2 h, the yield of the product **3a** was found to increase sharply up to 1.5 equiv of the additive used (Table 1, entries 12-14). Notably, DCC was substituted by EDC.HCl as the former led major problem of separation of the product from the reaction mixture due to the formation of water insoluble by-product dicyclohexyl urea (DCU) (Table 1, entry 15). Low yield was obtained when the reaction was carried out with coupling reagent HATU/TBTU/HBTU in the presence of the additive (Table 1, entries 16-18). Again, no product was found with PyBOP as coupling reagent in the presence of HOBt (Table 1, entry 19). Next, the effect of solvent on the yield of benzoazetinone **3a** was studied. Solvents such as DCM, DMF, pyridine, and NMM provided lower yield (Table 1, entries 20-23), whereas DIPEA was found to be a more effective base for the reaction (Table 1, entry 24). Overall, the optimized reaction condition seems to be the use of 1.5 equiv of EDC.HCl, 1.5 equiv of HOBt and 3.0 equiv of Et₃N in THF at room temperature (Table 1, entry 15).

To test the generality of the reaction, other substrates 2-(*N*-acyl)amino benzoic acids **2b-k** were reacted under the optimized reaction conditions, and *N*-acyl benzoazetinones **3b-k** were obtained in 58-80% yields (Table 2). In Table 2, it is observed that the substrates **2b** and **2f**, having benzoyl and pivaloyl group at the *N*-center, obtained lower yields of the

benzoazetinone derivatives **3b** and **3f**, respectively. This might be due to the steric effect exerted by the bulky group.

The structure of benzoazetinone derivatives **3** was determined from their analytical and spectral data exclusively (supporting information file).

However, when optimized conditions (Table 2, entry 15) were used with the substrates **1b** and **4**, the desired benzoazetines **5** and **6** were not found (Scheme 1). This might be due to the instability of the aforesaid benzoazetinone derivatives, which indicated the importance of acyl group.

MOLECULAR MODELING OF BENZOAZETINONES

Global optimization of benzoazetines was followed prior to flexible docking of these compounds onto the active site (heme binding site) of the target-model, CYP53A15. The use of properly minimized three-dimensional structure is a necessity for an effective assessment of flexible ligand-target interactions. We used semi-empirical procedure followed by *ab initio* procedure of Gaussian G03W for the purpose.^[32] Two-step procedures were necessary as only the semi-empirical method was seen to be ineffective for meeting the convergence criteria of some of these compounds (e.g. **3k**; Table 3). Again, application of *ab initio* method as sole scheme poses the problem of meeting convergence criteria. Energies of each of these structures are seen to be very large and negative, indicative of a well-optimized global minimal structure. The energy of **3g** is highly negative and may be due to the substitution of R³ by Br (Table 3).

High negative scores for site-specific docking of this group of compounds against the model structure indicate well-formed complexes. The nature of the substituent at R³-site of ligand seems to contribute to the complex formation and hence, the effectiveness of interactions. Bulky aromatic ring along with non-polar substitution at the site (Table 2) is seen to produce more negative docking scores (as seen in the case of **3i**; Table 3). For example, compounds **3g** to **3j** differ only by R³ substitutions. The non-polar and polar natures of R³-substituent are more in **3i** and **3g**, respectively. The former has the highest and the latter has the lowest docking score (Table 3).

HOMOLOGY MODELING OF FUNGAL TARGET

Model structure of CYP53A15 is highly optimized and validated using 4-point criteria^[33, 34] and judged by per residue RMSD comparison (Figure 1).

Accuracy in homology model depends on many factors such as choice of template, their alignment, loop optimization, and energy minimization of the initial model as obtained by Modeller software.^[36] Overall, per residue RMSD of the present model is seen to be improved in comparison with an earlier model PM0075149^[17] (that uses similar template set) against the reference template structure 4D6Z.pdb (Figure 1). We used high-resolution X-ray crystallographic structure 4D6Z.pdb instead of 4LXJ.pdb as the template. There are a few advantages associated with the former. First, it belongs to the same class (4-monooxygenase) as the query sequence (CYP53A15). Second, query sequence has a higher identity (26%) with 4D6Z_A than 4LXJ.pdb (19%). Third,

4LXJ.pdb, although belonging to the same genera, participates in demethylation reaction. Further, we used multiple templates' criteria^[36] as 4D6Z_A has missing residues. The missing region was modeled using the structural information of other relatively low-resolution template structures (1Z10.pdb and 4NY4.pdb), keeping the rest of the structural information from 4D6Z_A.

DOCKING STUDIES

To identify and understand the potential antifungal behavior of benzoazetinones, docking simulation and virtual screening were performed using Autodock 4.2 and vina 1.1.2 tools,^[37] respectively. Target (model structure of CYP53A15) and ligand were prepared for virtual screening using Autodock tools.^[37] The scores, thus, obtained are presented in Table 3. Figure 2 shows stabilizing interactions of CYP53A15 and one of these representative ligands (**3i**) at the heme-binding pocket. Ligand-protein interactions are largely stabilized by hydrogen bonding, and van der Waals, hydrophobic and π -alkyl interactions.^[38] In the heme-binding pocket of the target, **3i** is seen to establish a number of stabilizing interactions that include i] amide- π -stacking with Ala284; ii] alkyl and π -alkyl interactions with Val429 and Ala430, respectively; iii] hydrogen bonding with Gly426; iv] covalent bond with Phe108; and v] van der Waals' interactions with Thr288, Val425, Cys424, Phe108, Gln281, Leu255, and Glu433 (Figure 2).

Figure 3 (A) shows the docking complex between the target protein and the ligand **3i**, which has maximum interaction energy (Table 3). It is seen that the binding pocket is appropriately fits by the ligand **3i** with its hydrophobic group MeC₆H₄ directed deep near

the floor of the cavity. This region of the cavity is also seen to be hydrophobic [Figure 3 (B), SAS scale]. Interestingly, the methyl group of MeC₆H₄ (R³ substituent) is also in contact with the hydrophobic part of the pocket. Such hydrophobic stabilization is not possible with **3g**, **3h** and **3j** structures that have Br, OMeC₆H₄ and C₆H₅ groups, respectively. Thus, additional stabilization might be related to the methyl group in **3i** at its R³ site. Further, ligand structures **3a** to **3f** have hydrogen atom at the R³ site (Table 2). The docking scores of these ligands are much lower than that of **3i** except **3b**. The R⁵ substituent of **3i** and **3b** are Me and C₆H₅ group, respectively. Overall, it seems the hydrophobic nature of R³ and also R⁵ bring stability to the docking complex with higher effective contribution from the earlier.

CONCLUSIONS

In conclusion, we have successfully developed an inexpensive and efficient method for the synthesis of stable *N*-acyl benzoazetinones in moderate to good yields (58-85%) from easily available starting materials 2-(*N*-acyl)amino benzoic acids under mild conditions, which is simply intramolecular amidation. Here, both the EDC.HCl and corresponding by-product urea are water soluble so that the benzoazetinone derivatives can easily be isolated from the reaction mixture, i.e., the procedure is simple. Moreover, the *N*-acyl functional group present in the benzoazetinone derivatives can be further functionalized. These benzoazetinones undergo interactions in the heme binding site of CYP53A15, a fungal P450 isozyme. **3i** has the most effective interaction possibly due to hydrophobic stabilization and better packing at the interaction site. Hydrophobic nature of R³ substituent (also R⁵) helps to form a stable complex. The score of interaction not only

shows this list of compounds to be potential antifungal agents but also raises the possibility of development of potential antifungal agents specifically targeting the CYP53 class of P450.

Experimental Section

All chemicals and reagents used in current study were commercially available analytical or chemically pure grade reagents, unless otherwise indicated. Melting points were determined in open capillaries and are uncorrected. All the reactions were monitored by analytical thin-layer chromatography (TLC) using 0.25 mm E.Merk precoated silica gel plates (60F254). Silica gel (100-200 mesh) was used for chromatographic separation. All the ^1H NMR and ^{13}C NMR spectra were recorded using a model DPX400 spectrometer (TOP Spin 2.1 Ultra shieldTM) in $\text{CDCl}_3/\text{DMSO}-d_6$ and chemical shifts were reported in δ (ppm) units relative to the internal standard tetramethylsilane (TMS). LCMS spectra, GCMS spectra and HRMS spectra were recorded on QTRAP Applied Biosystem/Shimadzu Autosampler, Agilent 6890 series with 5973 Mass selective detector and Qtof Micro instrument respectively. CHN were recorded on a Perkin-Elmer 2400 series II CHN-analyzer.

General Synthetic Procedure for the Title Compounds 3

To a stirred solution of 2-Acetylamino-6-methoxy-benzoic acid **2a** (200 mg, 0.95 mmol) in dry THF (10 mL) was added 1-ethyl-3-(3-dimethylaminopropyl)carbodiimide hydrochloride (EDC.HCl) (274 mg, 1.43 mmol), 1-hydroxybenzotriazole (HOBt) (193 mg, 1.43 mmol) and triethylamine (0.4 mL, 2.85 mmol) at 0 °C. Then it was stirred at

room temperature for 2 h. The reaction mixture was diluted to 50 mL with ethyl acetate and then the organic phase was washed successively with water (2 x 15 mL), brine (2 x 10mL) and was dried over anhydrous Na₂SO₄. The organic phase was concentrated under reduced pressure to get the crude product which was purified by column chromatography over silica gel (100-200 mesh) with 2:3 ethylacetate/hexane (v/v) eluant to afford the benzoazetinone **3a** as pure product. Accordingly, other products **3b-k** were synthesized.

1-Acetyl-3-Methoxybenzo[B]Azet-2(1H)-One (**3a**)

Yield: 85%; white solid; m.p. 190 °C; ¹H NMR (400 MHz, CDCl₃) δ: 2.41 (s, 3H, COCH₃), 4.00 (s, 3H, OCH₃), 6.93 (d, *J* = 8.4 Hz, 1H, ArH), 7.09 (d, *J* = 8.0 Hz, 1H, ArH), 7.68 (t, *J* = 8.2 Hz, 1H, ArH); ¹³C NMR (100 MHz, DMSO-*d*₆) δ: 20.6, 56.2, 105.0, 110.2, 117.6, 137.3, 148.2, 155.2, 160.3, 160.7; HRMS (ESI) *m/z*: Calcd for C₁₀H₉NNaO₃ [M + Na]⁺: 214.0480; Found: 214.0286; LCMS *m/z*: 192.1 [M + H]⁺; Anal. Calcd. for C₁₀H₉NO₃: C, 62.82; H, 4.74; N, 7.33. Found: C, 62.69; H, 4.91; N, 7.19.

Optimization Procedure for Benzoazetinone

Chemical structures of benzoazetinones were drawn using Gauss View 3.0. Each of this structure was subjected to two successive optimization schemes. Semi-empirical, PM3 was used first, followed by *ab initio* HF/STO-3G* methods of Gaussian 03 package program. Lowest energy structure was stored for docking studies.

Homology Modeling

Three templates for CYP53A15 (UNIPROT ID B8QM33) were chosen using E-value and sequence identity criteria. Full length of 4D6Z_A (resolution 1.93 Å, UNIPROT ID P08684 and length 23-503) along with part of 1Z10_A (1.90 Å, UNIPROT ID P11509) and 4NY4_A (2.95 Å, UNIPROT ID P08684) were used to obtain the topology information for missing residues in the former using multiple template procedures of Modeler 9v11.^[36] Heteroatoms of template were transfer using advanced modeling method of Modeler. Five models were generated of which the best model was selected based on Discrete Optimized Protein Energy (DOPE) score.^[36] The model was refined using conjugate gradient energy minimization scheme of NAMD in presence of explicit water box for 5000 steps with an interval of 200 steps and thus a total of 25 frames were collected. Lowest potential energy frame was taken as final model.

Structural evaluation, validation and stereo chemical analyses of the model was done by PROCHECK, ANOLEA, ERRAT and VERIFY in SAVES v4 web server (<https://services.mbi.ucla.edu/SAVES/>).

Docking and Virtual Screening

Autodock 4.2^[37] of the Scripps Research Institute was used for docking and preparation of ligand and target protein respectively. To identify the interaction zone, we perform docking, at the site of one of the three heteroatom (Heme, GOL and PK9) at a time of the template. The target (CYP53A15) and one of our compounds (**3i**) were prepared with MGLtools. Gasteiger partial charges were added. Non-polar hydrogen atoms were merged and rotatable bonds were defined. The site of the target intended for docking was

placed in a grid box with appropriate dimension and center along with 0.375 Å grid spacing. Torsions were allowed to the long side chains of the amino acid residues in the vicinity of the ligand. Docking simulations were performed using the Lamarckian genetic algorithm using default parameters. Initial position, orientation, and torsions of the ligand were set randomly. The best interacting site (Heme binding pocket of active site) thus obtained was then used for docking of all of our compounds (Table 2) using virtual screening procedure of Vina 1.1.2 (May, 2011).^[39]

ACKNOWLEDGEMENTS

We thank UGC (New Delhi) for providing Shimadzu UV-Vis, FTIR and GCMS spectrometers. We also thank DST (New Delhi) for providing Bruker single crystal XRD and Thermo Scientific HRMS instruments under the DST-PURSE and DST-FIST programme respectively. We (IA & AD) are also grateful to The University of Burdwan for financial support under the University Level Research Assistance programme. AKB like to thank Prof. Anirvan Misra, Department of Chemistry, North Bengal University, for allowing us to use his Gaussian software.

REFERENCES

- [1] (a) Ceric, H.; Sindler-Kulyk, M.; Kovacevic, M.; Peric, M.; Zivkovic, A. *Bioorg. Med. Chem.* **2010**, *18*, 3053; (b) Webber, J. A.; Wheeler, W. J. In *Chemistry and Biology of β -Lactam Antibiotics*; (ed. Morin, R. B. and Gorman, M.); Academic Press: New York, **1982**, pp. 372-436; (c) Long, T. E.; Turos, E. *Curr. Med. Chem.* **2002**, *1*, 251; (d) Cromwell, N. H.; Philips, B. *Chem. Rev.* **1979**, *79*, 331; (e) De Kimpe, N. In

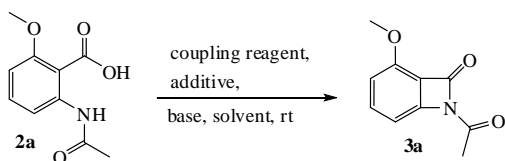
- Comprehensive Heterocyclic Chemistry II*; (ed. Padwa, A.); Elsevier Science, **1996**, Vol. 1B, pp. 508-545; (f) *Synthesis of β -Lactam Antibiotics*; (ed. Bruggink, A.); © Springer Science & Business Media Dordrecht, **2001**; (g) Sundberg, R. J. In *Comprehensive Heterocyclic Chemistry II*; (ed. Katritzky, A. R.; Rees, C. W. and Scriven, E. F. V.); Pergamon Press: Oxford, **1996**, p. 149; (h) Georg, G. I.; Ravikumar, V. T. *The Organic Chemistry of β -Lactams*; (ed. Georg, G. I.); VCH: New York, **1993**, pp. 295-368.
- [2] (a) Suffness, M. (Eds.); *Taxol Science and Applications*; CRC Press; Boca Raton, FL, USA: **1995**, pp. 379-415; (b) Bose, A. K.; Mathur, C.; Wagle, D. R.; Manhas, M. S. *Tetrahedron Symposium in Print* **2000**, 56, 5603; (c) Alcaide, B.; Almendros, P.; Aragoncillo, C. *Chem. Rev.* **2007**, 107, 4437.
- [3] Buynak, J. *Curr. Med. Chem.* **2004**, 11, 1951.
- [4] (a) Burnett, D. A. *Curr. Med. Chem.* **2004**, 11, 1873; (b) Clader, J. W. *J. Med. Chem.* **2004**, 47, 1.
- [5] Finke, P. E.; Shah, S. K.; Fletcher, D. S.; Ashe, B. M.; Brause, K. A.; Chandler, G. O.; Dellea, P. S.; Hand, K. M.; Maycock, A. L.; Osinga, D. G.; Underwood, D. J.; Weston H.; Davies, P.; Doherty, J. B. *J. Med. Chem.* **1995**, 38, 2449.
- [6] O'Driscoll, M.; Greenhalgh, K.; Young, A.; Turos, E.; Dickey, S.; Lim, D. V. *Bioorg. Med. Chem.* **2008**, 16, 7832.
- [7] Kanafani, Z. A.; Perfect, J. R. *Clinic. Infect. Dis.* **2008**, 46, 120.
- [8] Limper, A. H.; Knox, K. S; Sarosi, G. A.; Ampel, N. M.; Bennett, J. E.; Catanzaro, A.; Davies, S. F.; Dismukes, W. E.; Hage, C. A.; Marr, K. A.; Mody, C. H.; Perfect, J. R.; Stevens, D. A. *Am. J. Respir. Crit. Care Med.* **2011**, 183, 96.
- [9] Andriole, V. T. *Int. J. Antimicrob. Agents.* **2000**, 16, 317.

- [10] Giraud, F.; Guillon, R.; Logé, C.; Pagniez, F.; Picot, C.; Le Borgne, M.; Le Pape, P. *Med. Chem. Lett.* **2009**, *19*, 301.
- [11] Vanden, B. H.; Dromer, F.; Improvisi, I.; Lozano-Chiu, M.; Rex, J. H.; Sanglard, D. *Med. Mycol.* **1997**, *36*, 119.
- [12] Perfect, J. R. *Med. Myco.* **2009**, *47*, S324.
- [13] Masubuchi, M.; Ebiike, H.; Kawasaki, K. I.; Sogabe, S.; Morikami, K.; Shiratori, et. al. *Bioorg. Med. Chem.* **2003**, *11*, 4463.
- [14] Saha, S.; Priyadharshini, A.; Dhanasekaran, D.; Thajuddin, N.; Chandraleka, S.; Chandramohan, G.; Panneerselvam, A. *Comput. Boil. Med.* **2012**, *42*, 542.
- [15] Crešnar, B.; Petric, S. *Biochim. Biophys. Acta.* **2011**, *1814*, 29.
- [16] Kelly, S. L.; Kelly, D. E. *Phil. Trans. R. Soc.* **2013**, *368*, 1612.
- [17] Podobnik, B.; Stojan, J.; Lah, L.; ner, T. L.; Rozman, D.; Komel, R. *J. Med. Chem.* **2008**, *51*, 3480.
- [18] Sandanayaka, V. P.; Prashad, A. S.; Yang, Y.; Williamson, T.; Lin, Y. I.; Mansour, T. S. *J. Med. Chem.* **2003**, *46*, 2569.
- [19] Buynak, J. D.; Rao, A. S.; Fod, G. P.; Carver, C.; Adam, G.; Geng, B.; Bachmann, B.; Shobassy, S.; Lackey, S. *J. Med. Chem.* **1997**, *40*, 3423.
- [20] Bonneau, P. R.; Hasani, F.; Plouffe, C.; Malenfant, E.; Laplante, S. R.; Guse, I.; Ogilvie, W. W.; Plante, R.; Davidson, W. C.; Hopkins, J. L.; Morelock, M. M.; Cordingley, M. G. Deziel, R. *J. Am. Chem. Soc.* **1999**, *121*, 2965.
- [21] (a) Pitts, C. R.; Lectka, T. *Chem. Rev.* **2014**, *114*, 7930; and references there in.
(b) Banik, B. K.; Ghatak, A.; Becker, F. F. *J. Chem. Soc., Perkin Trans.* **2000**, *1*, 2179;
(c) Banik, B. K.; Becker, F. F. *Tetrahedron Lett.* **2000**, *41*, 6551; (d) Ng, S.; Banik, I.;

- Okawa, A.; Becker, F. F.; Banik, B. K. *J. Chem. Res.(S)* **2001**, 118; (e) Banik, B. K.; Samajdar, S.; Banik, I. *Tetrahedron Lett.* **2003**, 44, 1699; (f) Banik, B. K.; Adler, D.; Nguyen, P.; Srivastava, N. *Heterocycles* **2003**, 61, 101; (g) Banik, B. K.; Lecea, B.; Arrieta, A.; Cozar, A.; Cossio, F. P. *Angew. Chem. Int. Ed.* **2007**, 46, 3028. (h) Banik, B. K.; Aguilar, H.; Cordova, D. *Heterocycles* **2008**, 11, 2321.
- [22] (a) Fodor, L.; Csomos, P.; Holczbauer, T.; Kalman, A.; Csampai, A.; Sohar, P. *Tetrahedron Lett.* **2011**, 52, 224; (b) Janikowska, K.; Pawelska, N.; Makowiec, S. *Synthesis* **2011**, 1, 69; (c) Dubey, A.; Srivastava, S. K.; Srivastava, S. D. *Bioorg. Med. Chem. Lett.* **2011**, 21, 569; (d) Feroci, M.; Chiarotto, I.; Orsinib, M.; Inesi, A. *Chem. Commun.* **2010**, 46, 4121; (e) Keri, R. S.; Hosamani, K. M.; Shingalapur, R. V.; Reddy, H. R. S. *Eur. J. Med. Chem.* **2009**, 44, 5123; (f) Dekeukeleire, S.; D'hooghe, M.; Muller, C.; Vogt, D.; De Kimpe, N. *New J. Chem.* **2010**, 34, 1079; (g) Jarrahpour, A.; Zarei, M. *Molecules* **2006**, 11, 49; (h) Jarrahpour, A.; Khalili, D. *Tetrahedron Lett.* **2007**, 48, 7140; (i) Jarrahpour, A.; Ebrahimi, E. *Molecules* **2010**, 15, 515.
- [23] Burgess, E. M.; Milne, G. *Tetrahedron Lett.* **1966**, 7, 93.
- [24] Smalley, R. K.; Suschitzky, H.; Tanner, E. M. *Tetrahedron Lett.* **1966**, 7, 3465.
- [25] Chiu, S.-J.; Chou, C.-H. *Tetrahedron Lett.* **1999**, 40, 9271.
- [26] Olofson, R. A.; Vander Meer, R. K.; Stournas, S. *J. Am. Chem. Soc.* **1971**, 93, 1543.
- [27] Dai, W.-M.; Cheung, Y. K.; Tang, K. W.; Choi, P. Y.; Chung, S. L. *Tetrahedron* **1995**, 51, 12263.
- [28] Nowak, M. Malinowski, Z.; Jozwiak, A.; Fornal, E.; Blaszczyk, A.; Kontek, R. *Tetrahedron* **2014**, 70, 5153.

- [29] Kayarmar, R.; Nagaraja, G. K.; Bhat, M.; Naik, P.; Rajesh, K. P.; Shetty, S.; Arulmoli, T. *Med. Chem. Res.* **2014**, *23*, 2964.
- [30] Cioffi, C. L.; Dobri, N.; Freeman, E. E.; Conlon, M. P.; Chen, P.; Stafford, D. G.; Schwarz, D. M. C.; Golden, K. C.; Zhu, L.; Kitchen, D. B.; Barnes, K. D.; Racz, B.; Qin, Q.; Michelotti, E.; Cywin, C. L.; Martin, W. H.; Pearson, P. G.; Johnson, G.; Petrukhin, K. *J. Med. Chem.* **2014**, *57*, 7731.
- [31] Emenike, B. U.; Liu, A. T.; Naveo, E. P.; Roberts, J. D. *J. Org. Chem.* **2013**, *78*, 11765.
- [32] Alam, A.; Pal C.; Goyal, M.; Kundu, M. K.; Kumar, R.; Iqbal, M. S.; Dey, S.; Bindu, S.; Sarkar, S.; Pal, U.; Maiti, N. C. *Bioorg. Med. Chem.* **2011**, *19*, 7365.
- [33] Mondal, S.; Mondal, B.; Bandyopadhyay, A. K. *Int. J. Eng. Sci. Technol.* **2013**, *5*, 992.
- [34] Mondal, B.; Sen Gupta, P. S.; Roy, C.; Islam, R. N. U.; Hazra, N.; Bandyopadhyay, A. K. *Int. J. Pharm. Bio Sci.* **2016**, *7*, 406.
- [35] Humphrey, W.; Dalke, A.; Schulten, K. *J. mol. graphs.* **1996**, *29*, 33.
- [36] Webb, B.; Sali, A. *Curr. Protoc. Bioinformatics.* **2014**, *8*, 5.
- [37] Morris, G. M.; Huey, R.; Lindstrom, W.; Sanner, M. F.; Belew, R. K.; Goodsell, D. S.; Olson, A. J. *J. Comp. Chem.* **2009**, *16*, 2785.
- [38] Wang, H. C.; Yan, X. Q.; Yan, T. L.; Li, H. X.; Wang, Z. C.; Zhu, H. L. *Molecules.* **2016**, *21*, 1012.
- [39] Trott, O.; Olson, A. *J. Comp. Chem.* **2010**, *31*, 455.

Table 1. Optimization of reaction condition for the synthesis of benzoazetinone **3a**.

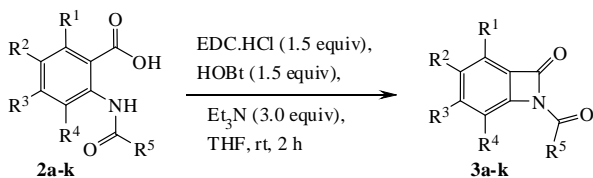


Entry	Coupling reagent (equiv)	Additive (equiv)	Base (equiv) ^a	Solvent ^a	Time (h)	Yield (%) ^b
1	HATU (1.5)	—	DIPEA (3.0)	DMF	12	15
2	HATU (1.5)	—	Et ₃ N (3.0)	DMF	12	25
3	HATU (1.5)	—	Py (3.0)	DMF	12	10
4	HATU (1.5)	—	Et ₃ N (3.0)	DCM	12	10
5	HATU (1.5)	—	Et ₃ N (3.0)	THF	12	45
6	HATU (2.0)	—	Et ₃ N (3.0)	THF	12	45
7	DCC (1.5)	—	Et ₃ N (3.0)	THF	12	17
8	EDC.HCl (1.5)	—	Et ₃ N (3.0)	THF	12	52
9	TBTU (1.5)	—	Et ₃ N (3.0)	THF	12	46
10	HBTU (1.5)	—	Et ₃ N (3.0)	THF	12	49
11	PyBOP (1.5)	—	Et ₃ N (3.0)	THF	18	n.r.
12	DCC (1.5)	HOBt (1.0)	Et ₃ N (3.0)	THF	2	70
13	DCC (1.5)	HOBt (1.5)	Et ₃ N (3.0)	THF	2	73
14	DCC (1.5)	HOBt (2.0)	Et ₃ N (3.0)	THF	2	73

15 ^c	EDC.HCl (1.5)	HOBt (1.5)	Et ₃ N (3.0)	THF	2	85
16	HATU (1.5)	HOBt (1.5)	Et ₃ N (3.0)	THF	2	58
17	TBTU (1.5)	HOBt (1.5)	Et ₃ N (3.0)	THF	2	53
18	HBTU (1.5)	HOBt (1.5)	Et ₃ N (3.0)	THF	2	50
19	PyBOP (1.5)	HOBt (1.5)	Et ₃ N (3.0)	THF	2	n.r.
20	EDC.HCl (1.5)	HOBt (1.5)	Et ₃ N (3.0)	DCM	2	60
21	EDC.HCl (1.5)	HOBt (1.5)	Et ₃ N (3.0)	DMF	2	37
22	EDC.HCl (1.5)	HOBt (1.5)	Py (3.0)	THF	2	32
23	EDC.HCl (1.5)	HOBt (1.5)	NMM (3.0)	THF	2	40
24	EDC.HCl (1.5)	HOBt (1.5)	DIPEA (3.0)	THF	2	76

^aDry solvents and bases were used; ^bIsolated yield of the compound **3a**; ^cOptimized reaction conditions; n.r. = No reaction

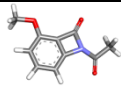
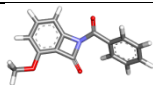
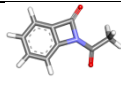
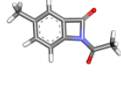
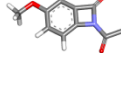
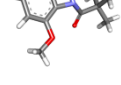
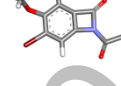
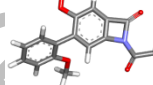
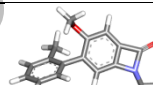
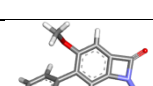
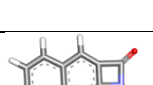
Table 2. Synthesis of *N*-acyl benzoazetines **3**.



Entry	R ¹	R ²	R ³	R ⁴	R ⁵	Compound	Yield (%) ^a
1	OMe	H	H	H	Me	3a	85
2	OMe	H	H	H	Ph	3b	60
3	H	H	H	H	Me	3c	72
4	H	Me	H	H	Me	3d	78
5	H	OMe	H	H	Me	3e	79
6	H	H	H	OMe	^t Bu	3f	58
7	H	OMe	Br	H	Me	3g	73
8	H	OMe	<i>o</i> -OMeC ₆ H ₄	H	Me	3h	69
9	H	OMe	<i>o</i> -MeC ₆ H ₄	H	Me	3i	70
10	H	OMe	Ph	H	Me	3j	74
11	H	-CH=CH-CH=CH-		H	Me	3k	80

^aIsolated yield of the compounds **3a-k**

Table 3. Details of optimization and docking score of benzoazetines.

Compounds	Structure	Energy [∞]	Docking score [§]
3a		-654.50	-28.56
3b		-892.67	-34.44
3c		-542.10	-28.14
3d		-580.66	-31.51
3e		-654.50	-28.98
3f		-770.23	-31.54
3g		-3198.71	-29.45
3h		-993.67	-32.34
3i		-919.83	-37.38
3j		-881.25	-34.86
3k		-654.29	-31.53

[∞] hartree (a.u.); [§] kJ mol⁻¹

Scheme 1. Reaction of substrates **1b** and **4** under optimized condition.

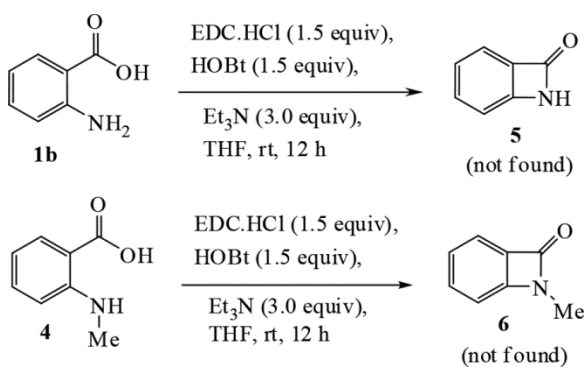


Figure 1. Per residue RMSD of 4D6Z (Blue line; Template, used as reference), present model (red line) and PM0075149 (green). Alignment of three structures were done using STRAMP structural alignment in VMD interface.^[35]

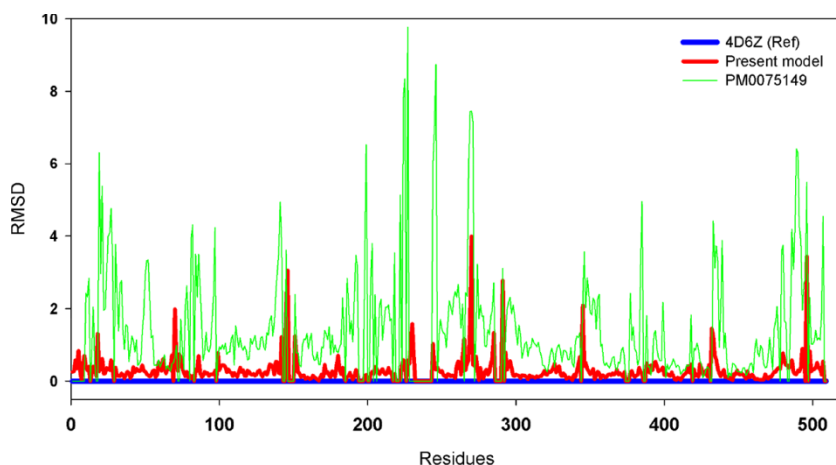


Figure 2. 2D model of interactions between the ligand **3i** with target protein; for clarity, only interacting residues are displayed. Presence of blue sphere around residues indicates accessibility.

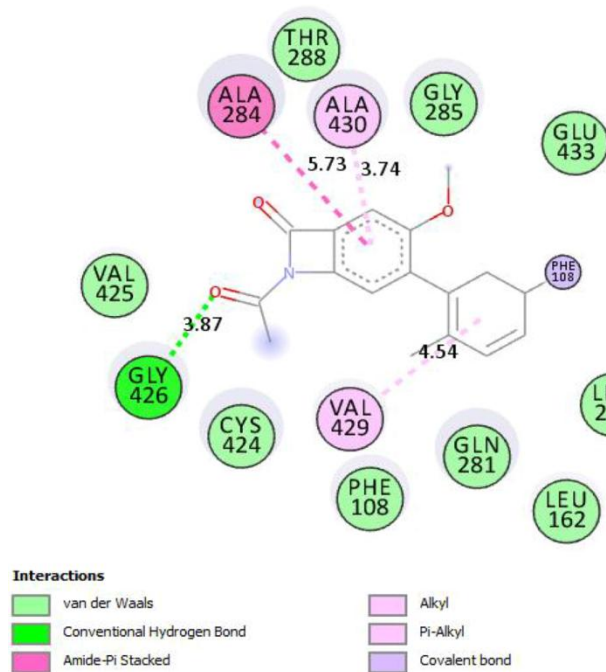


Figure 3. (A) Docking complex of model structure of CYP53A15 and geometry optimized ligand, **3i**; (B) Ligand (red) binding pocket, interacting residues, and their solvent accessible surface (SAS) are shown along with SAS scale; (C) A copy of ligand at identical orientation as it is present in the binding pocket to guess positions of invisible atoms. Residues labels, written in blue color are not visible in the front view.

